Z. Phys. C - Particles and Fields 33, 363-375 (1987)

Zeitschrift für Physik C Particles and Fields

Universality of Hadron Jets in Soft and Hard Particle Interactions at High Energies

A.M. Baldin[1], L.A. Didenko[1], V.G. Grishin[1], A.A. Kuznetsov[1], Z.V. Metreveli[2]

[1] Laboratory of High Energies, Joint Institute for Nuclear Research, Head Post Office P.O. Box 79, SU-101000 Moscow, USSR
[2] Institute of High Energies Physics, Tbilisi State University, University St. 9, SU-380086 Tbilisi 86, USSR

Received 14 February 1986; in revised form 16 September 1986

Abstract. Hadron jet production is studied in soft $\pi^- p$ and cumulative $\pi^- C$ interactions at a 40 GeV/c momentum. The collective characteristics of jets and the form of the quark and diquark fragmentation into charged pions and neutral strange particles are analyzed. The results obtained are compared to analogous data for e^+e^- and $\nu(\tilde{\nu})p$ interactions. The hadron jet properties are also studied by means of relativistic invariant variables - the squared relative 4-velocities $b_{ik} = -\left(\frac{P_i}{m_i} - \frac{P_k}{m_k}\right)^2$. The results obtained show that quark (diquark) fragmentation proceeds in a similar manner in soft hadron-hadron collisions, cumulative interactions on light nuclei, e^+e^- annihilation and deep inelastic $\nu(\tilde{\nu})p$ scattering. In the relativistically invariant variables the fragmentation function is similar for the hadronization of quarks and diquarks and it does not matter whether they are knocked out of usual hadrons or multiquark systems.

1. Introduction

Nowadays a great amount of experimental information is collected on hadron jet production in different types of interaction: e^+e^- annihilation, deep inelastic lepton scattering on nucleons, soft and hard hadron-hadron collisions. A comparative analysis of all data shows that the behaviour of the most important characteristics of the jets in these interactions has universal properties [1-5]:

The universality of jets, segregate objects of multiple particle production, is interpreted as a result of the single production mechanism of quarks (gluons) knocked out of the parental hadron and transforming into hadrons, the products of the reactions.

A direct check of this mechanism is to observe and to study the jets produced in relativistic nuclear collisions. Varying the size of the nucleus (studying the dependence of jet production on the atomic weight), one can in principle find out the characteristic size, on which the jet is formed, and also the influence of nuclear matter on jet production. The study of hadron jet production in cumulative processes is of particular interest as in these processes quarks (gluons) are knocked out of the multiquark configurations of nuclei. Experiments on the study of the limiting fragmentation of nuclei [6-8] and on the investigation of the deep inelastic scattering of muons and electrons on nuclei [9-11] point to the existence of such configurations.

In this paper hadron jet production is studied in cumulative $\pi^- C$ interactions at a 40 GeV/c momentum. The results obtained are compared with data on $\pi^- p$ interactions at the same energy ($P = 40$ GeV/c) and for e^+e^-, $\nu(\tilde{\nu})p$ collisions.

Possible diagrams of the hadron jet production in these processes are presented in Fig. 1. The analysis of soft hadron-hadron interactions [3-5] has shown that the production of two hadron jets, collimated in the c.m.s. in the direction of motion of the primary hadron and in the opposite one, is observed in these interactions. One can assume that the jets are produced in the forward (backward) hemisphere in the $\pi^- p$ c.m.s. due to the fragmentation of noninteracting valence quarks (diquarks) belonging to the composition of initial particles.

Similar representations were used in the study of hadron jet production in cumulative $\pi^- C$ interactions. The production of hadron jets was assumed to

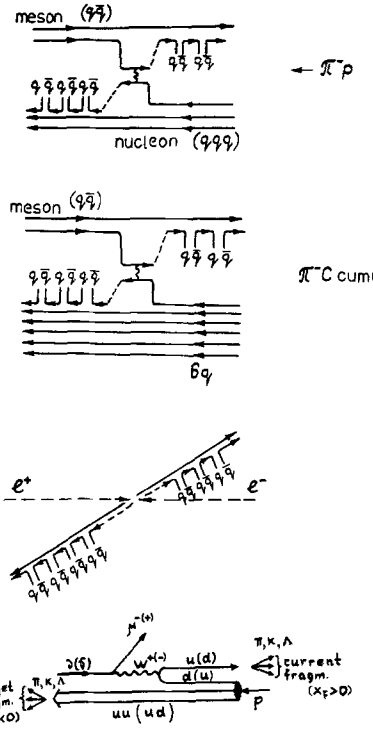

Fig. 1. Diagrams of different processes

be due to the fragmentation of noninteracting $\bar{u}(d)$ quarks from the incident π^- meson in the forward hemisphere in the c.m.s. of cumulative interactions and due to the fragmentation of quarks and diquarks from the multiquark configurations of nuclei in the backward hemisphere. Assuming that in the studied events the length of quark formation to a jet is larger than the size of the carbon nucleus, of which the quark is knocked out, one can expect that the hadron jet properties in nuclei are similar to those in hadron-hadron, e^+e^- and $\nu(\tilde{\nu})p$ interactions.

The investigation of hadron jet properties has been made on a statistics of 14,000 $\pi^- p$ and 8,791 $\pi^- C$ events selected on pictures from the 2 m propane bubble chamber exposed to 40 GeV/c mesons at the Serpuknov accelerator. The technique of event selection and experimental data processing has been described previously [12–14]. In the analysis of $\pi^- p$ interactions diffraction processes were excluded*.

2. Hadron Jet Properties in $\pi^- p$ Interactions

2.1. Characteristics of the Jets

The study of the hadron jet production in $\pi^- p$ interactions has been performed in the collision c.m.s. ($E_{\text{c.m.s.}} \equiv \sqrt{S} = 8.76$ GeV).

Figure 2 presents the energy (in the c.m.s.) dependence of the average values of the variable $\langle S \rangle$ for e^+e^- annihilation [15–19]. The same figure shows the value of $\langle S \rangle$ obtained for $\pi^- p$ interactions [5] at 40 GeV/c and for $K^\pm p$ and pp collisions at higher energies [20]. As seen from the figure, the average value of $\langle S \rangle$ for $\pi^- p$ events agrees, within the experimental errors, with the existing energy dependence of $\langle S \rangle$ for e^+e^- and soft hadron-hadron interactions.

The average multiplicity of charged particles (n_{ch}) in $\pi^- p$ [5] interactions is compared to that in e^+e^- annihilation. Furthermore, the average longitudinal ($\langle P_\parallel \rangle$) and transverse ($\langle P_\perp \rangle$) momenta of particles relative to the jet axis compared for the two processes.

These data are shown in Figs. 3 and 4, respectively. As seen from the figures, the considered characteristics coincide, within the experimental errors, for both types of interaction at the same energies in the c.m.s.

Figure 5a and b presents the distribution of π^+ mesons in the forward hemisphere and of π^- mesons in the backward hemisphere over the variable $x_F = 2P_\parallel^*/\sqrt{S}$ ($P_\parallel^*$ is the projection of the momentum P^* on the jet axis) in the $\pi^- p$ c.m.s. [5]. They are compared with analogous distributions of charged pions for e^+e^- annihilation at an energy of 7.4 GeV [21]. In the forward hemisphere the distributions are in agreement, within the experimental errors, for both processes whereas in the backward hemisphere the x_F distribution of π^- mesons falls faster for $\pi^- p$ events than for e^+e^- annihilation. As noted in the introduction, one can assume that the production of the hadron jets in the backward hemisphere in the $\pi^- p$ c.m.s. is due to the fragmentation of uu or ud diquarks belonging to the composition of the initial proton whereas in e^+e^- annihilation the fragmentation of quarks is considered.

Therefore the difference of the two distributions in the backward hemisphere of $\pi^- p$ events may be due to the differences of the quark and diquark fragmentation functions into pions.

In connection with this it is of interest to compare the experimental data on $\pi^- p$ interactions with similar characteristics on $\nu(\tilde{\nu})p$ collisions, in which according to the simplest scheme (Fig. 1) of the quark-parton model, the particles, emitted to the forward hemisphere in the c.m.s. of secondary hadrons, are assumed to be the products of the fragmentation of $u(d)$ quarks, and the particles emitted to the backward hemisphere – the products of the fragmentation of $uu(ud)$ diquarks.

* The event was considered to be a diffraction one if, at least, one charged secondary particle had $|x_F| \geqq 0.8$ ($x_F = 2P_\parallel^*/\sqrt{S}$)

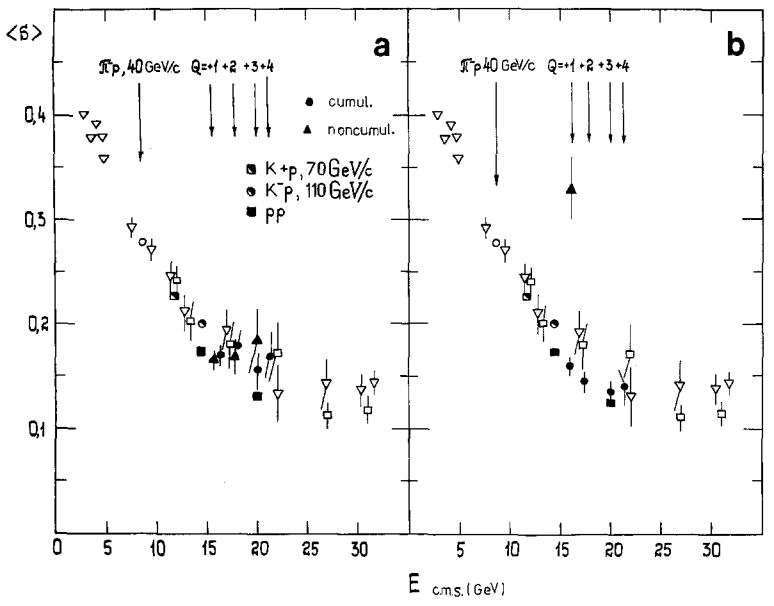

Fig. 2a, b. The dependence of the average values of $\langle S \rangle$ for different types of interactions on the c.m.s. energy: ▽, □ – in e^+e^- annihilation; ○, ◪, ◔, ■ – in $\pi^- p$, $K^+ p$, $K^- p$, pp interactions, respectively; **a** for the hadron jets emitted forward and **b** backward in the c.m.s. in cumulative (●) and noncumulative (▲) $\pi^- C$ collision

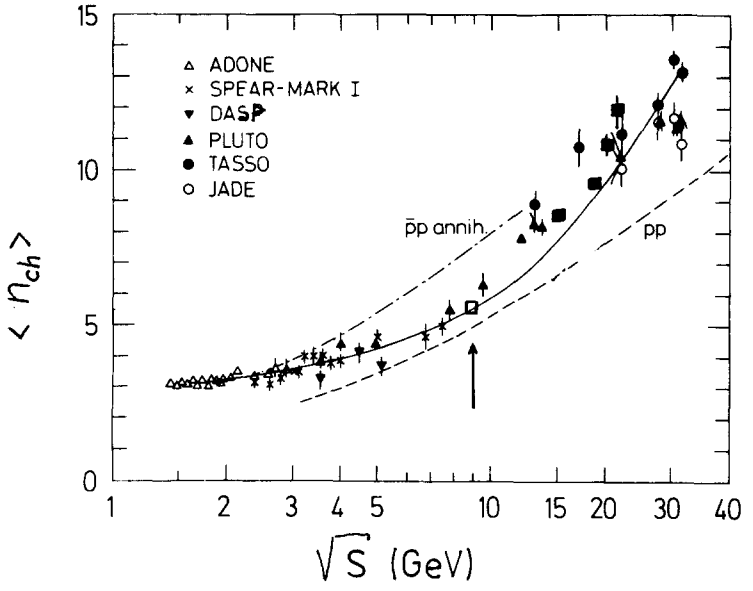

Fig. 3. The dependence of the average multiplicity of charged particles, $\langle n_{ch} \rangle$, on the c.m.s. energy $(\sqrt{S})$ in e^+e^- collisions in $\pi^- p$ (□) and cumulative $\pi^- C$ interactions (■). The solid curve is the prediction of QCD for e^+e^- annihilation

2.2. *Fragmentation of Quarks and Diquarks into Pions*

Comparing the diagrams of $\pi^- p$ and $\nu(\tilde{\nu})p$ interactions (Fig. 1) and assuming that the light quarks $\bar{u}$ and d interact with the same probability, the following relations can be written for the fragmentation function

$$D(x_F) = 1/N_{ev}(dN/dx_F)$$

($x_F = P_{\parallel}^*/P_{\max}$, $P_{\parallel}^*$ is the projection of the momentum on the reaction axis):

$$D_{\pi^- p}^{\pi^\pm}(x_F) = \tfrac{1}{2} D_{vp}^{\pi^\mp}(x_F) + \tfrac{1}{2} D_{\tilde{\nu}p}^{\pi^\pm}(x_F)$$
for $x_F \geqq 0.1$★ (1)

$$D_{\pi^- p}^{\pi^\pm}(x_F) = \tfrac{1}{3} D_{vp}^{\pi^\pm}(x_F) + \tfrac{2}{3} D_{\tilde{\nu}p}^{\pi^\pm}(x_F)$$
for $x_F \leqq -0.1$. (2)

The charge-conjugate relations for the quark fragmentation

$$D_{\bar{u}}^{\pi^+}(x_F) = D_u^{\pi^-}(x_F)$$

★ In the region $|x_F| \leqq 0.1$ in $\pi^- p$ collisions the influence of qq interactions is assumed to be significant

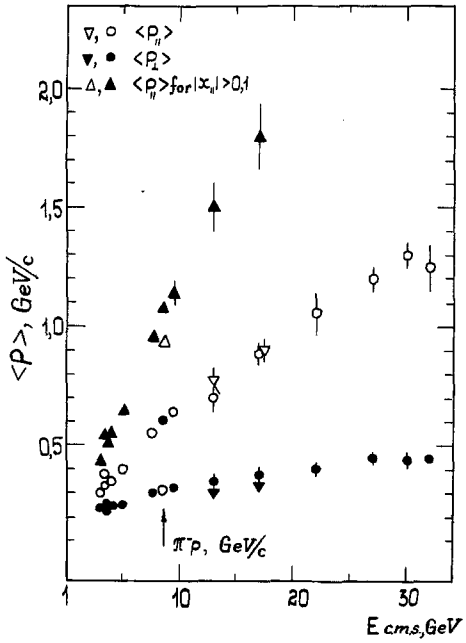

Fig. 4. The dependence of the average transverse and longitudinal momenta of secondary particles relative to the jet axis on the c.m.s. energy for e^+e^- annihilation: ●, ○ - PLUTO Collaboration; ▼, ▽ - TASSO Collaboration. ▲ - average values of the longitudinal momentum of secondary particles for $|x_F| \geqq 0.1$. The values of $\langle P_\perp \rangle$ and $\langle P_\parallel \rangle$ corresponding to $\pi^- p$ interactions at 40 GeV/c are denoted by the arrow. ▲ and △ correspond to the average values of $\langle P_\parallel \rangle$ for $|x_F| \geqq 0.1$ obtained with and without taking diffraction processes into account

and

$$D_{\bar{u}}^{\pi^-}(x_F) = D_u^{\pi^+}(x_F)$$

are taken into account in (1).

The function of the fragmentation of quarks, $D^{\pi^+}(x_F)$, into π^+ mesons in $\pi^- p$ events [5] is compared with the function obtained from the $\nu(\tilde{\nu})p$ data [22] according to (1) (see Fig. 6a). In Fig. 6b we compare the function of the fragmentation of diquarks, $D^{\pi^-}(x_F)$, into π^- mesons in $\pi^- p$ interactions and the $D^{\pi^-}(x_F)$ function obtained from $\nu(\tilde{\nu})p$ collisions according to (2). The distribution for the two processes agrees well, within the experimental errors, except for the region $|x_F| \leqq 0.1$, where the contribution from interacting quarks in $\pi^- p$ collisions is substantial.

Approximating the fragmentation functions by the expression

$$D^{\pi^\pm}(x_F) = A \exp(-B \cdot |x_F|), \tag{3}$$

we find that the values of the parameters A and B are approximately equal for both processes (Table 1).

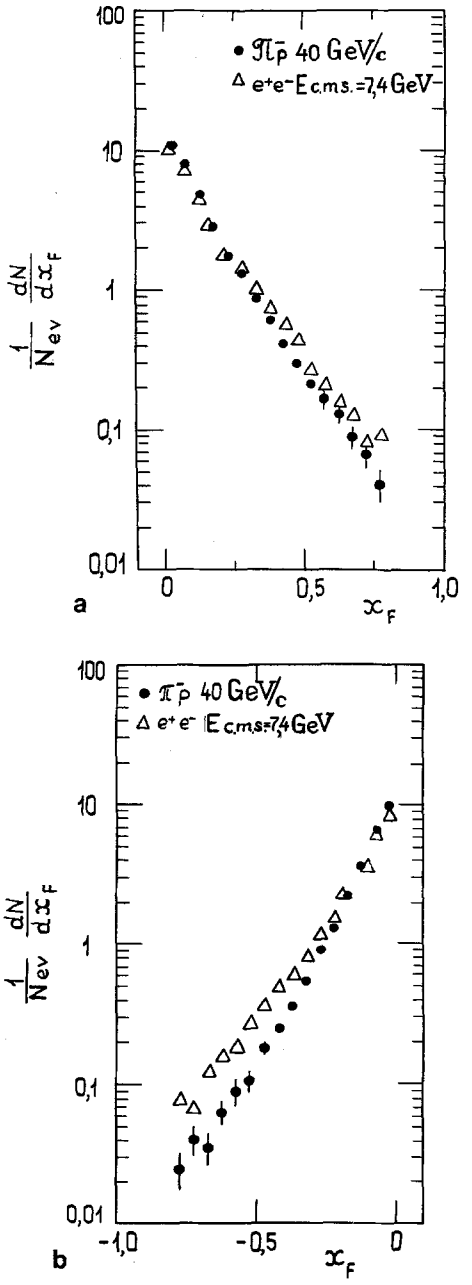

Fig. 5a, b. The x_F distributions of charged particles relative to the jet axis: △ - for e^+e^- annihilation ($\sqrt{S} = 7.4$ GeV); ● - for $\pi^- p$ interactions ($\sqrt{S} = 8.7$ GeV): **a** for π^+ mesons in the forward hemisphere, **b** for π^- mesons in the backward hemisphere

2.3. *Fragmentation of Quarks and Diquarks into Strange Particles*

To compare the fragmentation of quarks and diquarks into neutral K^0 mesons and Λ^0 hyperons for different types of interaction, we used the $\frac{1}{\beta}\frac{d\sigma}{dx_E}$ scaling functions [23]. The analysis of the e^+e^- data was performed by means of these functions. Here x_E

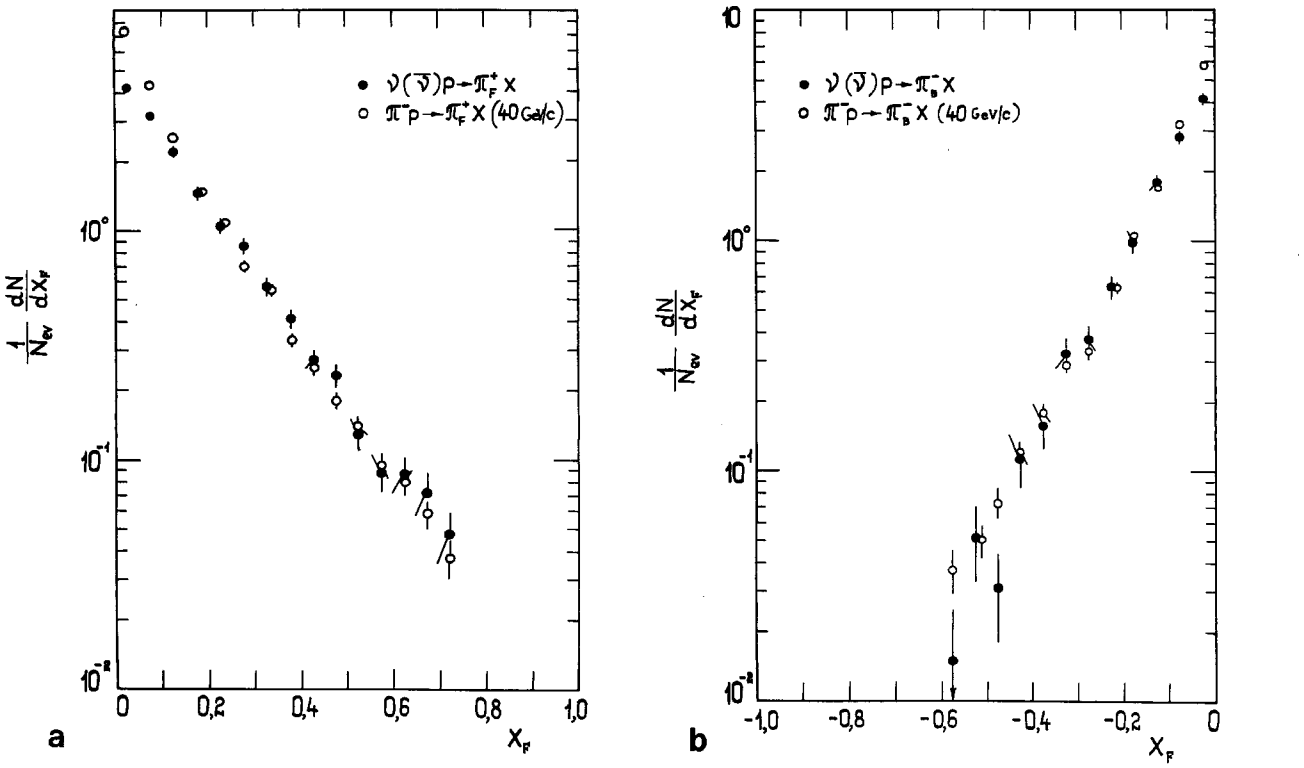

Fig. 6. a Fragmentation functions: ● $\frac{1}{2}D^{\pi^-}_{vp}+\frac{1}{2}D^{\pi^+}_{\bar{v}p}$, ○ - $D^{\pi^+}_{\pi^-p}$ for $x_F>0$. **b** Fragmentation functions: ● $\frac{1}{3}D^{\pi^-}_{vp}+\frac{2}{3}D^{\pi^-}_{\bar{v}p}$, ○ - $D^{\pi^-}_{\pi^-p}$ for $x_F<0$

$=\frac{2E^*}{\sqrt{S}}$, $\beta=\frac{P^*}{E^*}$; P^*, E^* are the momentum and energy of the hadron in the c.m.s. 753 K^0_s mesons ($K^0_s\to\pi^+\pi^-$) and 345 Λ^0-hyperons ($\Lambda^0\to p\pi^-$) were used for the analysis in $\pi^- p$ interactions [24, 25].

The x_E dependence of the $1/\beta$ $(d\sigma/dx_E)$ functions for K^0 mesons and Λ^0 hyperons in the fragmentation of quarks in $\pi^- p$ [5] (forward hemisphere) and e^+e^- collisions [26, 27] is shown in Figs. 7 and 8 (the distributions are normalized to the area in the region $x_E\geqq 0.15$ for K^0 mesons in e^+e^- interactions and $x_E\geqq 0.25$ for Λ hyperons in $\pi^- p$ collisions). As seen from the figures, the distributions for both processes coincide within the experimental errors. The $\frac{1}{\beta}\frac{d\sigma}{dx_E}$ function for K^0 mesons and Λ hyperons can be approximated by the dependence

$$\frac{1}{\beta}\frac{d\sigma}{dx_E}=A\exp(-Bx_E). \tag{4}$$

The slope B in $\pi^- p$ interactions equals 10 ± 1 and 8 ± 3 for the two types of particles, respectively. These values are approximately equal to those for e^+e^- annihilation ($B\simeq 8$) [27].

The value of the ratio $\lambda_s=\langle n_K\rangle/\langle n_\pi\rangle$, characterizing the pickup probability of strange and nonstrange quarks from the sea, is 0.18 ± 0.02 for $\pi^- p$ interactions in the region $x_E=0.2\div0.5$ which is in agreement with the e^+e^- data ($\lambda_s\simeq 0.17$) [26, 27].

In Figs. 9 and 10 we show the x_E dependence of the $1/\beta$ $(d\sigma/dx_E)$ functions for K^0 mesons and Λ

Table 1. Approximation $D^{\pi^\pm}(x_F)$ by the expression-$A\exp(-B|x_F|)$

	Type of process	Region x_F	A	B	χ^2/n
$\pi^-(x_F<0)$	$\nu(\bar{\nu})p$	$-0.425\leqq x_F\leqq -0.125$	5.5 ± 0.6	9.4 ± 0.5	4.9/ 7
$\pi^-(x_F<0)$	$\pi^- p$	$-0.425\leqq x_F\leqq -0.125$	5.1 ± 0.2	9.0 ± 0.2	4.8/ 7
$\pi^+(x_F>0)$	$\nu(\bar{\nu})p$	$0.125\leqq x_F\leqq 0.725$	4.6 ± 0.3	5.5 ± 0.2	9.1/10
$\pi^+(x_F>0)$	$\pi^- p$	$0.125\leqq x_F\leqq 0.725$	4.7 ± 0.2	6.8 ± 0.1	12.9/10
$\pi^-(x_F>0)$	$\nu(\bar{\nu})p$	$0.225\leqq x_F\leqq 0.775$	5.5 ± 0.4	4.9 ± 0.2	13.3/12
$\pi^-(x_F>0)$	$\pi^- p$	$0.225\leqq x_F\leqq 0.775$	4.2 ± 0.2	4.4 ± 0.1	62.6/12

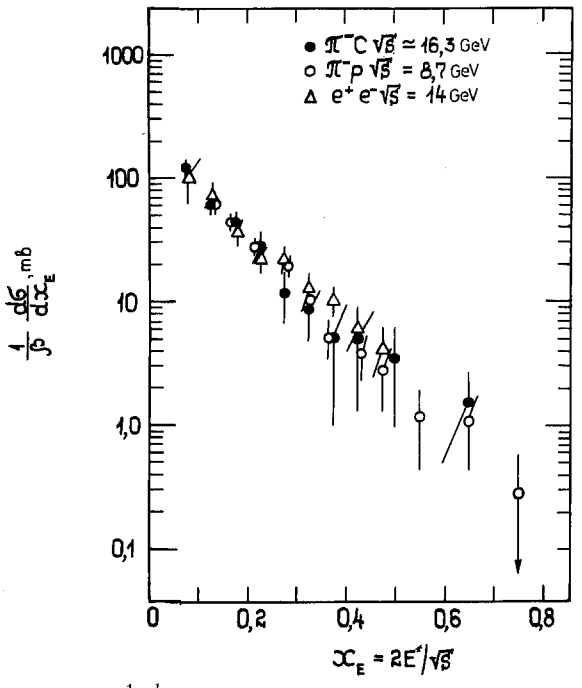

Fig. 7. The $\frac{1}{\beta}\frac{d\sigma}{dx_E}$ distribution for K^0 mesons produced in the forward hemisphere in the c.m.s. of cumulative $\pi^- C$ (●) ($\sqrt{S}=16.3$ GeV), $\pi^- p$ (○) ($\sqrt{S}=8.7$ GeV) and e^+e^- (△) ($\sqrt{S}=14$ GeV) interactions

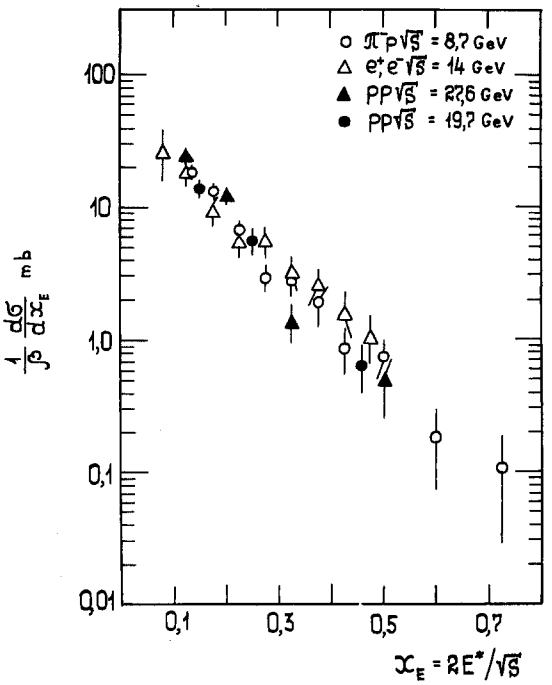

Fig. 9. The $\frac{1}{\beta}\frac{d\sigma}{dx_E}$ distribution for K^0 mesons produced in the backward hemisphere: ○ – for $\pi^- p$ interactions ($\sqrt{S}=8.7$ GeV); △ – for e^+e^- annihilation ($\sqrt{S}=14$ GeV); ▲, ● – for pp interactions at $\sqrt{S}=27.6$ and 19.7 GeV

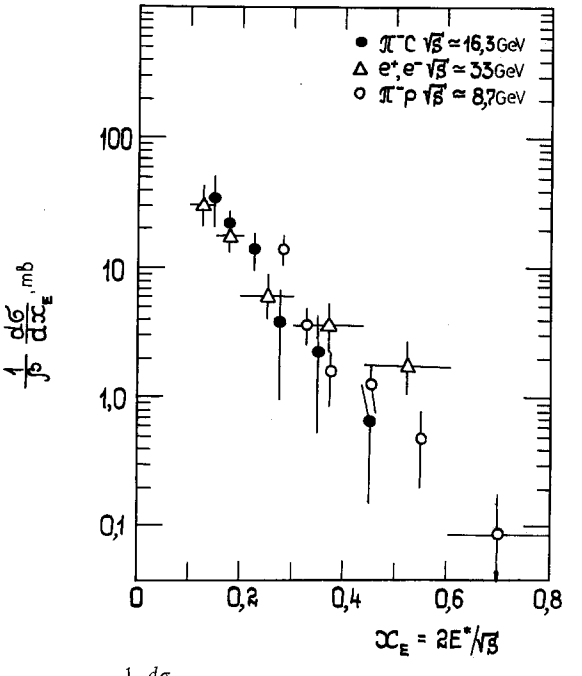

Fig. 8. The $\frac{1}{\beta}\frac{d\sigma}{dx_E}$ distribution for Λ hyperons produced in the forward hemisphere in the c.m.s. of cumulative $\pi^- C$ (●) ($\sqrt{S}=16.3$ GeV), $\pi^- p$ (○) ($\sqrt{S}=8.7$ GeV) and e^+e^- (△) ($\sqrt{S}=33$ GeV) interactions

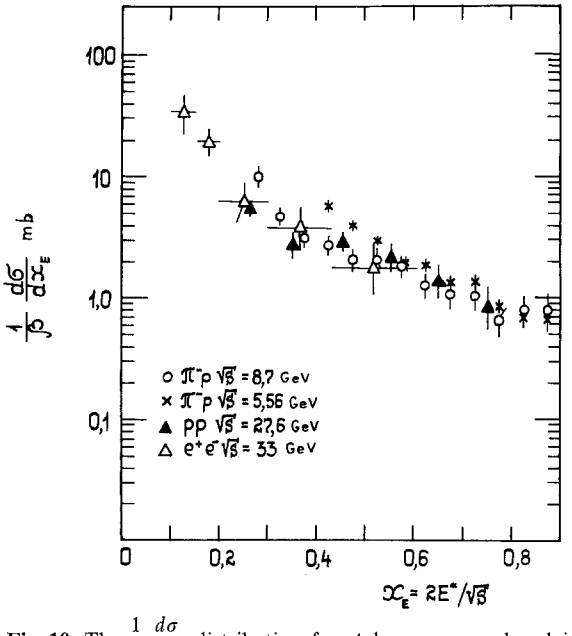

Fig. 10. The $\frac{1}{\beta}\frac{d\sigma}{dx_E}$ distribution for Λ hyperons produced in the backward hemisphere: ○, × – for $\pi^- p$ interactions at $\sqrt{S}=8.7$ and 5.56 GeV, ▲ – for pp interactions ($\sqrt{S}=27.6$ GeV), △ – for e^+e^- annihilation ($\sqrt{S}=33$ GeV)

hyperons produced in the fragmentation processes of diquarks in $\pi^- p$ [5] (backward hemisphere) and pp interactions from 16 [28] to 405 GeV/c [29, 30]. The same figures present the normalized data for e^+e^- collisions.

The distributions for neutral kaons in hadron-hadron interactions in the region $x_E \leqq 0.5$ do not differ, within the experimental errors ($\sim 30\%$), from the similar distribution in e^+e^- annihilation. The approximation of these distributions by the dependence (4) for $\pi^- p$ interactions yields $B=9\pm1$ in agreement with the e^+e^- data. The result obtained shows that the functions of the fragmentation of quarks and diquarks into neutral kaons in the region $x_E \leqq 0.5$ do not differ from one another within the experimental errors.

The values of the slope B in the $1/\beta\ (d\sigma/dx_E)$ distribution for Λ hyperons in $\pi^- p$ interactions at 40 and 16 GeV/c [5] in the backward hemisphere in the c.m.s. are respectively equal to 3.6 ± 0.4 and 4.4 ± 0.3 which is approximately 2 times smaller than in e^+e^- annihilation. Even though the x_E region is different, this probably means that the fragmentation functions of quarks and diquarks into Λ hyperons have a different x_E dependence. However, to make more definite conclusions, more accurate e^+e^- data are needed, especially in the region $x_E > 0.6$.

2.4. Average Charge of the Hadron Jets

It is of interest to define the average charge of the hadron jets produced in the forward and backward hemispheres in the c.m.s. and to compare it with the expected value from the quark-parton models.

If one neglects the difference between $\bar{u}$ and d quark interactions and assumes that valence quarks and diquarks fragment independently, the average charge of the jets emitted forward in the c.m.s. [31–33]:

$$\langle Q\rangle_f = \tfrac{1}{2}Q(\bar{u}) + \tfrac{1}{2}Q(d) + \langle Q_s\rangle = -0.5. \quad (5)$$

For the jets emitted backward in the c.m.s.

$$\langle Q\rangle_b = \tfrac{1}{3}Q(uu) + \tfrac{2}{3}Q(ud) + \langle Q_s\rangle \simeq 0.83, \quad (6)$$

where $\langle Q_s\rangle$ is the average charge of the sea quarks cancelling the colour of the fragmenting quark or diquark. To select the hadron jet with the quantum numbers of the fragmenting quark (diquark) with large probability, the average charge $\langle Q\rangle$ was defined depending on the value of $x=\sum_i |x_{F_i}|$, (Fig. 11) where summation is performed over all charged particles in the jet. In the region of large x values $x \geqq 0.8$, the average charge of the jets in the forward and backward hemisphere turned out to be close to the expected values of $\langle Q\rangle = -0.5$ and 0.83, respectively.

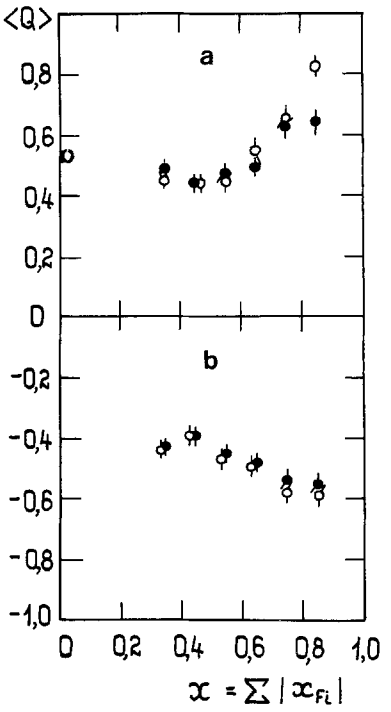

Fig. 11a, b. The average charge $\langle Q\rangle$ dependence on $x=\sum_i |x_{F_i}|$ in the events with $n_{ch} \geqq 4$ for $\pi^- p$ interactions: **a** in the backward hemisphere; **b** in the forward hemisphere. Full circles are the $x=\sum_i |x_{F_i}|$ values and $\langle Q\rangle$'s are determined for all the particles in the jet. Open circles are the x values and $\langle Q\rangle$'s are determined for the particles with $|x_{F_i}| \geqq 0.1$

Thus, summarizing briefly the study of the hadron jet properties produced in soft $\pi^- p$ interactions at a 40 GeV/c momentum, one can draw the following main conclusions:

1. In soft $\pi^- p$ interactions the production of two hadron jets is observed which can be considered to be due to the fragmentation of noninteracting valence quarks (forward hemisphere in the c.m.s.) and diquarks (backward hemisphere in the c.m.s.).

2. The functions of the fragmentation of quarks and diquarks into pions and strange particles in soft $\pi^- p$ interaction coincide, within experimental errors, with similar functions in e^+e^- and $\nu(\tilde{\nu})p$ collisions.

3. Hadron Jet Properties in $\pi^- C$ Interactions

To study the production of hadron jets in $\pi^- C$ collisions, multinucleon interactions with the total charge of secondary particles $Q=+1, +2, +3, +4$ were selected. For each group of multinucleon interactions with charge Q the analysis was performed in the c.m.s. of incident π^- meson and the cor-

responding number of interacting nucleons, $\langle \nu_N \rangle$ [34, 35]. The energy of the collision was defined according to the formula

$$E_{\text{c.m.s.}} \equiv \sqrt{S} \simeq \sqrt{2\nu_N m_N E_\pi} \tag{7}$$

with m_N the nucleon mass and E_π the energy of incident pion.

The cumulative events were selected using the variable β_i [7]

$$\beta_i = (E_i - P_{\|_i})/m_N, \tag{8}$$

where E_i and $P_{\|_i}$ are the energy and longitudinal momentum in the laboratory system. According to the established selection criteria, an event is assumed to be cumulative if a $\pi^{\pm}$-meson with $\beta_i \geqq 0.6$ [36] or a proton with $\beta_i \geqq 1$ is registered in it. However, the hadronization of quarks from the multiquark states of nuclei can occur so that none of the particles has the value of β_i outside the kinematical limit of pion-nucleon collisions whereas the sum of all β_i in the jet, produced due to the hadronization of quarks, is larger than 1.

$$\beta_0 = \sum_i \beta_i \geqq 1.0. \tag{9}$$

Thus, cumulative interactions were selected according to the condition (9). A group of particles, emitted backward in the c.m.s. of $(\pi^- \nu_N)$ interactions and satisfying the condition (9), was assumed to be a cumulative jet. The fraction of cumulative events thus selected was $\sim 18\,\%$ of all $\pi^- C$ interactions.

3.1. Jet Characteristics

Figure 2 presents the average values of $\langle S \rangle$ versus $E_{\text{c.m.s.}}$ for the secondary particle jets, emitted in the direction of motion of the primary pion and in the opposite direction, in cumulative ($\beta_0 \geqq 1.0$) and non-cumulative ($\beta_0 < 1.0$) events. The particles with $|x_{F_i}| = 2 \cdot |P_{\|}^*|/E_{\text{c.m.s.}} \geqq 0.05$ are assigned to jets. As seen from the figure, for both jets in cumulative $\pi^- C$ interactions the value of $\langle S \rangle$ agrees with the e^+e^- data at the same energies in the c.m.s. In noncumulative events, however, there is a disagreement with the data on e^+e^- interactions for the hadron jets produced in the fragmentation region of the target nucleus, this shows evidence for another mechanism of their production.

In Fig. 3 we show the energy dependence of the average multiplicity of charged particles in e^+e^- annihilation in the c.m.s. [16–19]. The average values of $\langle n_{\text{ch}} \rangle$ for cumulative events with $\beta_0 \geqq 1.0$ versus energy in the c.m.s. are given in the same figure. The $\langle n_{\text{ch}} \rangle$ multiplicity in cumulative processes increases with increasing $\sqrt{S}$ and coincides, within the experimental errors, with the $\langle n_{\text{ch}} \rangle$ value for e^+e^- interactions at equal energies.

3.2. Characteristics of Charged Particles in the Jets

Figure 12 shows the transverse momentum squared distributions of charged particles relative to the jet axis in cumulative $\pi^- C$ interactions with $Q = +1$ and e^+e^- annihilation. These $dN/dP_\perp^2$ distributions are similar for both types of interaction considered.

Figure 13 presents the distributions of secondary particles in the forward and backward hemispheres in the c.m.s. of cumulative $\pi^- C$ interactions with $Q = +1$ over $x_{\|} = 2P_{\|}/E_{\text{c.m.s.}}$, where $P_{\|}$ is the longitudinal momentum of particles relative to the jet axis.

From the figure one can see that the distribution of particles in the jets, emitted in the direction of motion of the primary meson, in cumulative $\pi^- C$ interactions coincide with the corresponding distribution in e^+e^- collisions. However, for the particles produced in the fragmentation region of the nucleus, the $x_{\|}$ distribution differs strongly from the corresponding distribution of charged particles in e^+e^- annihilation. This can be due to the differences of the initial states of interacting objects which lead to different compositions of secondary particles in the final state and, consequently, to distinctions in their phase space distributions. Therefore it would be

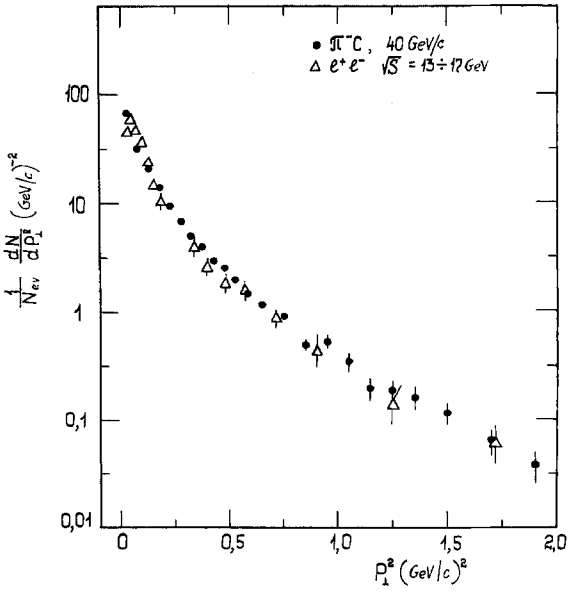

Fig. 12. The transverse momentum squared distribution of charged particles relative to the jet axis: • – for cumulative $\pi^- C$ interactions ($Q = 1$), △ – for e^+e^- annihilation at $\sqrt{S} = 13 \div 17$ GeV

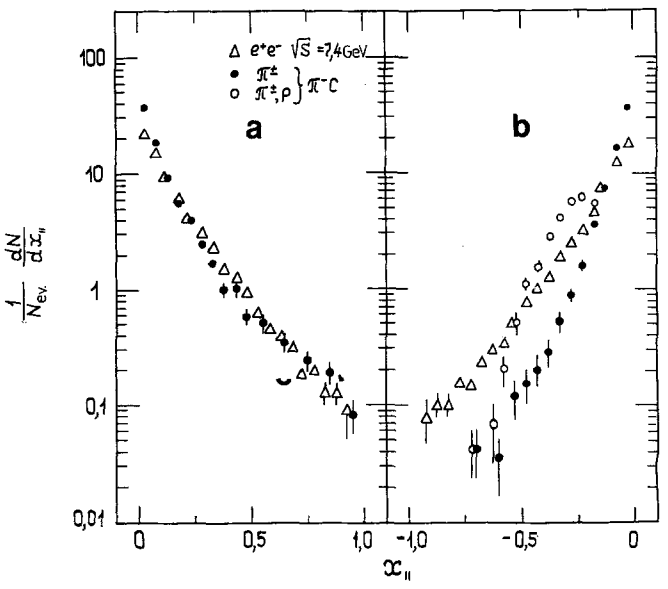

Fig. 13a, b. The $x_{\parallel}$ distribution of charged particles in the jets emitted forward **a** and backward **b** in the c.m.s. of cumulative $\pi^- C$ interactions with $Q=+1$

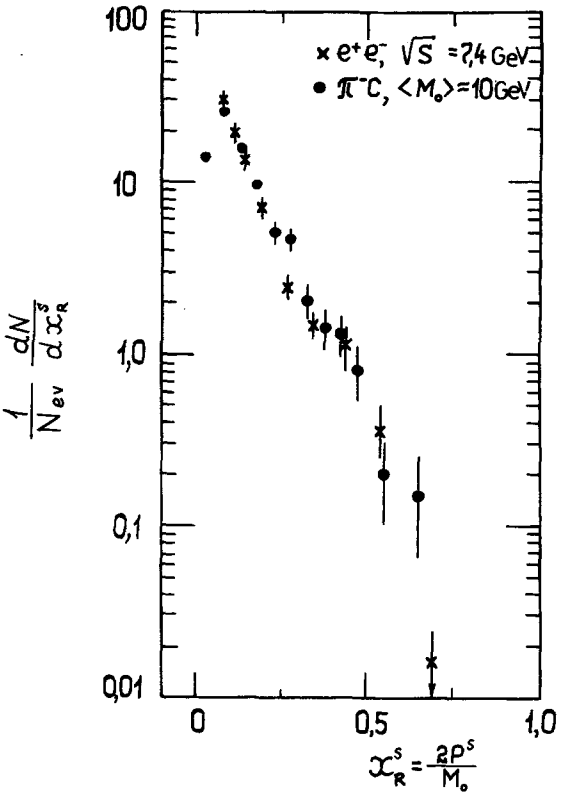

Fig. 14. The x_R^s distribution of pions produced in cumulative $\pi^- C$ collisions with $Q=+1$ in their rest frame at $\langle M_0\rangle=10$ GeV (backward hemisphere); × - the same distribution of pions in the e^+e^- c.m.s. at $E_{\text{c.m.s.}}=7.4$ GeV

interesting to compare identical systems of secondary particles in the final state (in this case the meson subsystems) in their rest frame. With this aim the events with two identified protons were selected from cumulative $\pi^- C$ interactions with $Q=+1$. The protons were excluded from the analysis. The energy of the remaining meson subsystem, $\langle M_0\rangle$, was equal to 10 GeV. Figures 14 and 15 illustrate the distributions of charged pions over the variables $x_R^s = 2P^s/M_0$ and

$$y_{\parallel}^s = \tfrac{1}{2}\ln((E^s+P_{\parallel}^s)/(E^s-P_{\parallel}^s)),$$

where P^s and E^s are the total momentum and energy of pions in their rest frame; $P_{\parallel}^s$ is the projection of the momentum P^s on the jet axis. These distributions agree, within the experimental errors, with the corresponding distribution of pions in e^+e^- annihilation.

3.3. Quark and Diquark Fragmentation into Strange Particles

550 K_s^0 mesons ($K_s^0\to\pi^+\pi^-$) and 294 Λ^0 hyperons ($\Lambda^0\to p\pi^-$) were used for the analysis [37].

Figures 7 and 8 present the $\frac{1}{\beta}\frac{d\sigma}{dx_E}$ function versus x_E for K^0 mesons and Λ hyperons produced in the fragmentation processes of quarks (forward hemisphere in the c.m.s.) in cumulative $\pi^- C$ interactions [38]. The normalized x_E distributions of K^0 mesons and Λ hyperons in $\pi^- p$ and e^+e^- in-

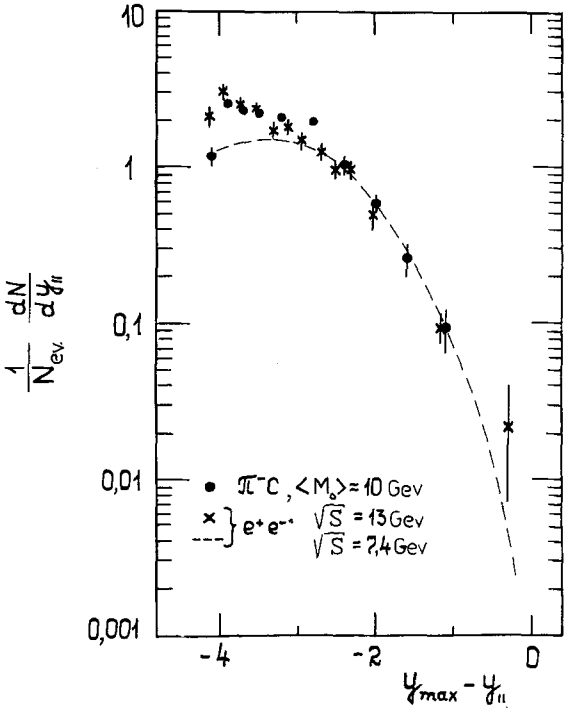

Fig. 15. The $y_{\parallel}^s$ distribution of pions produced in cumulative $\pi^- C$ interactions with $Q=+1$ in their rest frame at $\langle M_0\rangle=10$ GeV (backward hemisphere); ×, - - - - the same distributions of pions in the e^+e^- c.m.s. at $E_{\text{c.m.s.}}=13$ and 7.4 GeV, respectively

teractions are shown in the figures for comparison. As seen, the presented functions in the interactions under study are similar within the experimental errors. The approximation of these distributions by the dependence (4) for cumulative $\pi^- C$ interactions yields $B_{K^0}=9\pm2$ and $B_\Lambda=13\pm4$ (Table 2). They coincide, within the experimental errors, with values of B for $\pi^- p$ and e^+e^- interactions.

To compare the properties of K^0 mesons and Λ hyperons, produced in the target-nucleus fragmentation region in cumulative processes, with the $\pi^- p$ and e^+e^- data, we have selected a subsystem consisting of mesons and one baryon [38]. Then the production of Λ hyperons and K^0 mesons in the backward hemisphere in the rest frame of the selected subsystem can be considered to be due to the fragmentation of uu, ud and dd diquarks from the multiquark states of the carbon nucleus. The energy of the selected subsystem of secondary particles, $\langle M_0\rangle$, is 12.3 GeV.

Figures 16 and 17 show the $\frac{1}{\beta}\frac{d\sigma}{dx_E^s}$ function versus x_E^s for K^0 mesons and Λ hyperons produced in the target-nucleus fragmentation region in cumulative $\pi^- C$ interactions with $Q=+1,+2$. Here, $x_E^s=2E^s/M_0$ and E^s is the energy of particles in the rest frame of the subsystem M_0. From the figures one can see that the presented $\frac{1}{\beta}\frac{d\sigma}{dx_E^s}$ distributions for strange particles in the x_E^s region for cumulative $\pi^- C$, $\pi^- p$ and e^+e^- interactions are in agreement within the experimental errors. The values of the parameters B_{K^0} and B_Λ equal to 8 ± 4 and 5.2 ± 0.7, obtained by approximating these distributions by the dependence (4), agree, within the experimental

Table 2. Values of the Parameter B

Type of particles, Type of events	Forward hemisphere in the c.m.s.	Region of approximation	Backward hemisphere in the c.m.s.	Region of approximation
K^0-mesons $\pi^- C$-cumul.	9 ± 2	$x_E\geqq0.1$	$8\ \pm4$	$x_E^s\geqq0.15$
K^0-mesons $\pi^- p$, 40 GeV/c	10 ± 1	$x_E\geqq0.15$	$9\ \pm1$	$x_E\geqq0.15$
Λ-hyperons $\pi^- C$-cumul.	13 ± 4	$x_E\geqq0.15$	5.2 ± 0.7	$x_E^s\geqq0.2$
Λ-hyperons $\pi^- p$, 40 GeV/c	8 ± 3	$x_E\geqq0.3$	3.6 ± 0.4	$x_E\geqq0.3$
Λ-hyperons $\pi^- p$, 16 GeV/c [28]	10 ± 1	$x_E\geqq0.45$	4.4 ± 0.3	$x_E\geqq0.45$
K^0, Λ-particles e^+e^-	~8	$x_E\geqq0.1$	-	-

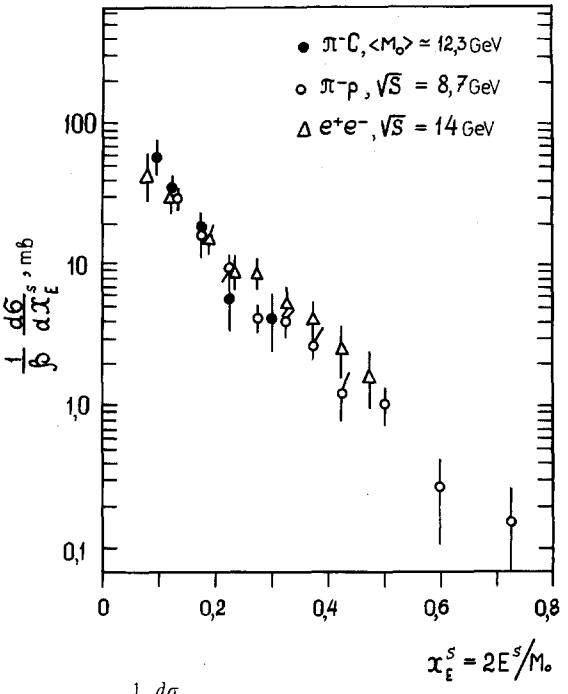

Fig. 16. The $\frac{1}{\beta}\frac{d\sigma}{dx_E^s}$ distribution for K^0 mesons produced in the backward hemisphere in the rest frame of the selected subsystem (M_0) in cumulative $\pi^- C$ interactions (•) ($\langle M_0\rangle=12.3$ GeV), in the c.m.s. of $\pi^- p$ (○) ($\sqrt{S}=8.7$ GeV) and e^+e^- (△) ($\sqrt{S}=14$ GeV) interactions

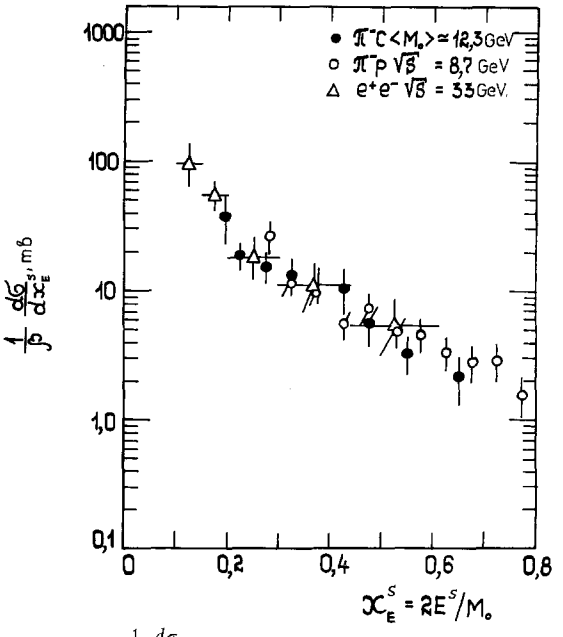

Fig. 17. The $\frac{1}{\beta}\frac{d\sigma}{dx_E^s}$ distribution for Λ hyperons in the backward hemisphere in the rest frame of the selected subsystem (M_0) in cumulative $\pi^- C$ interactions (•) ($\langle M_0\rangle=12.3$ GeV), in the c.m.s. of $\pi^- p$ (○) ($\sqrt{S}=8.7$ GeV) and e^+e^- (△) ($\sqrt{S}=33$ GeV) interactions

errors, with those for the $\pi^- p$ data. For Λ hyperons produced in the fragmentation processes of diquarks in $\pi^- p$ and cumulative $\pi^- C$ interactions, the values of the parameter B are smaller than those for $e^+ e^-$ annihilation, however.

From this section we conclude that single quark fragmentation functions are similar within errors for $e^+ e^-$ annihilation and forward jets in cumulative $\pi^- C$ and soft $\pi^- p$ collisions. The same holds for diquark fragmentation in backward jets in cumulative $\pi^- C$ and soft $\pi^- p$ collisions. From these similarities, it can be concluded that the hadron jets in pion-carbon interactions are mainly formed outside the nucleus.

4. Description of the Hadron Jet Properties in Relative 4-Velocity Space

To stude the hadron jet production, the standard variables sphericity (S) and thrust (T), are commonly used:

$$S=\tfrac{3}{2}(\sum_i P_{\perp i}^2/\sum_i |\mathbf{P}_i|^2) \tag{10}$$

$$T=(\sum_i |P_{\|_i}|/\sum_i |\mathbf{P}_i|) \tag{11}$$

where $\mathbf{P}_i$ are the momenta of secondary particles in the c.m.s. of colliding objects; $P_{\perp_i}$ and $P_{\|_i}$ are the transverse and longitudinal momenta of particles relative to some axis. Such an axis, for which $\sum_i P_{\perp_i}^2$ is minimal or $\sum_i |P_{\|_i}|$ is maximal in the determination of the values, respectively, is considered the jet axis.

However, the variables S and T are not Lorentz-invariant, and their values depend strongly on the reference frame. These facts should be taken into account in the analysis of experimental data and, in particular, in the study of the hadron jet properties in hadron-nucleus and nucleus-nucleus collisions. It is very difficult to define the c.m.s. in each individual case (i.e., versus the number of interacting nucleons of the nucleus) for such types of interaction.

Thus, to analyze the hadron jet properties in these interactions, a new method, based on a relativistically invariant description of multiple processes in relative 4-velocity space, has been proposed [39-41]

$$b_{ik}=-\left(\frac{P_i}{m_i}-\frac{P_k}{m_k}\right)^2=2\left[\frac{(P_i P_k)}{m_i m_k}-1\right]. \tag{12}$$

Here P_i and P_k are 4-momenta, m_i and m_k are the masses of primary and secondary particles. In this method a jet is considered as a cluster of hadrons with relatively small values of b_{ik}. A unit four-dimensional vector is used as a jet axis:

$$V=\sum_i u_i/\sqrt{(\sum_i u_i)^2} \quad \text{where } u_i=P_i/m_i. \tag{13}$$

Summation is performed over all particles from the selected group of particles. The distribution of the particles in the jet is analyzed by means of the variable

$$b_k=-(V-u_k)^2. \tag{14}$$

The above definition of the jet axis corresponds to a minimal value of $\sum_k b_k$ for the jet particles. The $(V-u_{\mathrm{I}})^2$ and $(V-u_{\mathrm{II}})^2$ distributions of the jets relative to the reaction axis

$$\mathrm{I}+\mathrm{II}\to 1+2+\ldots, \tag{15}$$

where indices I and II refer to primary particles, can be analyzed.

As will be shown below, the new method of invariant description of the hadron jet properties has advantages in the study of jet production in nuclear interactions. To select the particles belonging to a jet, the variable x_i was used [40], which is determined in a relativistically invariant manner. For the $\mathrm{I}+\mathrm{II}\to i+\ldots$ reaction the following designations are introduced:

$$x_{pi}=\frac{m_i(u_i u_{\mathrm{II}})}{m_{\mathrm{I}}(u_{\mathrm{I}} u_{\mathrm{II}})} \quad \text{and} \quad x_{ti}=\frac{m_i(u_i u_{\mathrm{I}})}{m_{\mathrm{II}}(u_{\mathrm{I}} u_{\mathrm{II}})}. \tag{16}$$

where $u_i=P_i/m_i$ is the 4-velocity of a secondary particle, $u_{\mathrm{I}}=P_{\mathrm{I}}/m_{\mathrm{I}}$ and $u_{\mathrm{II}}=P_{\mathrm{II}}/m_{\mathrm{II}}$ are the 4-velocitites of an incident π^- meson and a target nucleon, respectively. The pions with $x_{pi}\geqq 0.1$ and $x_{ti}\leqq 0.1$ belong to the jet produced in the beam fragmentation region and the pions with $x_{ti}\geqq 0.1$ and $x_{pi}\leqq 0.1$ to the jet produced in the target fragmentation region.

Figure 18 shows the b_k distribution of π^- mesons relative to the axis of the jets produced in the beam and target fragmentation regions of $\pi^- p$ interactions. A similar distribution of π^- mesons in pp collisions at $P=205$ GeV/c is also presented [42] (the data have been obtained using a hydrogen bubble chamber at FNAL). One can see that the distributions coincide within the experimental errors, i.e. in relative 4-velocity space the fragmentation of quarks and diquarks into pions is of the same character. Furthermore, the distribution obtained does not depend on the energy of the collision over an energy range of $40\div 205$ GeV/c.

Figure 19 illustrates the b_k distributions of π^- mesons in the jets produced in the target and beam

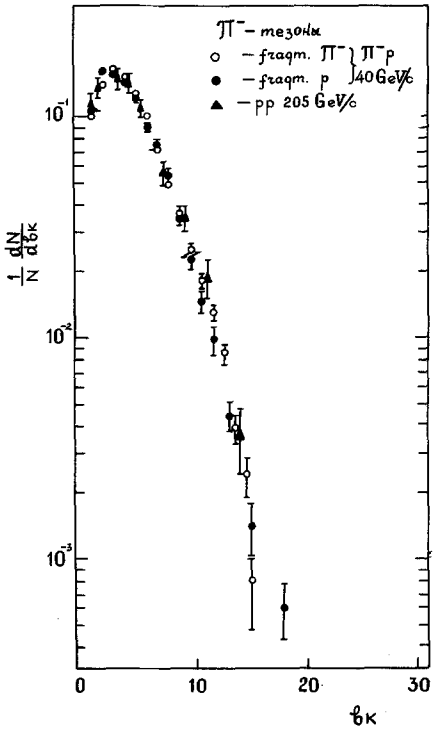

Fig. 18. The distribution of π^- mesons over b_k calculated relative to the axis of the jets produced in the fragmentation regions of incident pion (○) and proton (●) in $\pi^- p$ interactions. (▲) – the same distribution for pp collisions at $P=205$ GeV/c

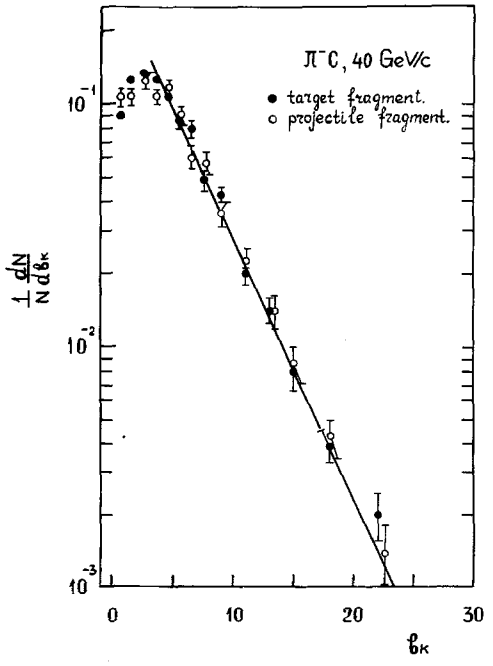

Fig. 19. The distribution of π^- mesons over b_k calculated relative to the axis of the jets produced in $\pi^- C$ interactions in the target (●) and beam (○) fragmentation region

fragmentation regions. These distributions are also in agreement within the experimental errors.

The b_k distribution of π^- mesons in the jets produced in the target fragmentation region of $\pi^- C$ interactions at $P=40$ GeV/c and of pp collisions at $P=205$ GeV/c are compared in Fig. 20. These distributions are similar as well.

Table 3 presents the average values of b_k for the different types of interaction. These values are small ($b_k \simeq 4$) ($b_{\text{II}}=570$ is the total interval in $\pi^- p$ collisions at $P=40$ GeV/c) and do not depend, within the errors, on the type and primary energy of interaction over the considered range of energies.

From this section we conclude:

1. Quark fragmentation and diquark fragmentation look the same in the new variable b_k.

2. The b_k distribution is the same at 40 and 205 GeV/c (scales).

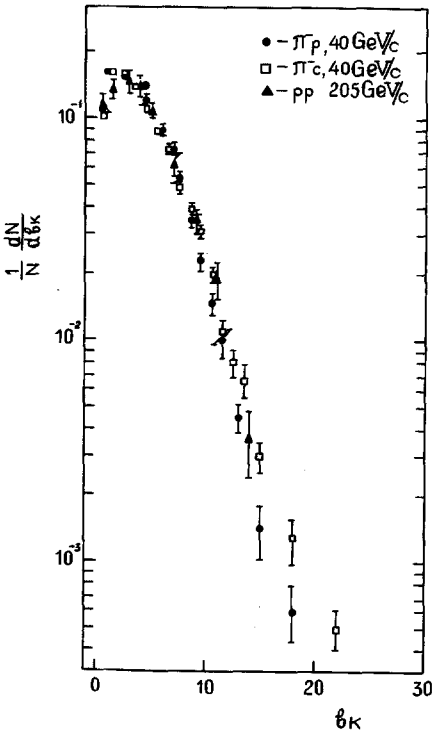

Fig. 20. The distribution of π^- mesons over b_k calculated relative to the axis of the jets produced in the target fragmentation region: (●) – $\pi^- p$, (□) – $\pi^- C$ interactions at 40 GeV/c and (▲) – pp collisions at $P=205$ GeV/c

Table 3. Average values of the b_k variables for π^- mesons

Region of jet production	$\pi^- p$	$\pi^- C$	pp
Beam fragmentation	4.2 ± 0.1	4.2 ± 0.1	4.5 ± 0.1
Target fragmentation	4.1 ± 0.1	4.4 ± 0.1	4.5 ± 0.1

3. No difference can be observed for hadron jets in $\pi^- C$ interactions from quark or diquark fragmentation jets in soft $\pi^- p$ interactions. This confirms the conclusion from Sect. 3, but now on the basis of the combined information from quark and diquark fragmentation.

5. Conclusions

From the analysis performed one can draw the following main conclusions:

1. In relativistic nuclear interactions the production of two-hadron jets is observed which are collimated in the direction of motion of colliding objects in their c.m.s. (i.e. in the beam and target fragmentation regions).

2. The main properties of the hadron jets are similar, within the experimental errors, to those observed in soft and hard hadron-hadron collisions and $e^+ e^-$ annihilation.

3. The functions of the fragmentation of quarks and diquarks into hadrons in relativistic hadron-nucleus interactions coincide, within the experimental errors, with the corresponding functions in soft hadron-hadron and $e^+ e^-$ collisions.

4. The hadron jets in cumulative hadron-nucleus interactions are mainly formed outside the nucleus.

5. In relative 4-velocity space the b_k distributions of secondary particles relative to the jet axis in different types of interaction are similar and do not depend on energy ($E = 40 \div 205$ GeV/c) both in the target and in the beam fragmentation regions. Thus, the new property of multiple processes, which does not depend on energy and the quark system composition, characterizing the dynamics of quark hadronization has been established in a relativistically invariant approach.

Acknowledgements. In conclusion the authors are grateful to the staff of the 2 m Propane Bubble Chamber Collaboration for their help in obtaining the experimental material and useful discussions.

References

1. M. Jacob: XXII. Int. Conf. on High Energy Phys., Leipzig, 19-25, 1984, Vol. 2, p. 150
2. M. Basile et al.: Nuovo Cimento **58A**, 193 (1980); **65A**, 414 (1981); **65A**, 400 (1981); **67A**, 244 (1982); **67A**, 53 (1982)
3. R. Gottgens et al.: Nucl. Phys. **B178**, 392 (1981)
4. M. Barth et al.: Nucl. Phys. **B192**, 289 (1981)
5. V.G. Grishin et al.: JINR, P1-81-542, Dubna (1981); JINR, P1-82-252, Dubna (1982); JINR, P1-83-306, Dubna (1983); Yad. Fiz. **37**, 915 (1983); Yad. Fiz. **38**, 967 (1983); Yad. Fiz. **40**, 936 (1984); Yad. Fiz. **41**, 684 (1985); JINR, P1-85-259, Dubna (1985)
6. A.M. Baldin: ECHAYA **8**, 429 (1977)
7. V.S. Stavinsky: ECHAYA **10**, 949 (1979); JINR, P2-80-767, Dubna, (1980)
8. V.G. Gavrilov, G.A. Leksin: Elementary Particles. X School of ITEF, M., Energoizdat, I, p. 46, (1983)
9. J.J. Aubert et al.: Phys. Lett. **123B**, 275 (1983)
10. A. Bodek et al.: Phys. Rev. Lett. **50**, 1431 (1983)
11. I.A. Savin: Proc. VI. Int. Seminar on High Energy Physics Problems, JINR, D1, 2-81-728, Dubna, p. 223, (1981)
12. BBCDSSTTU-BW Collaboration Phys. Lett.: **39B**, 371 (1972)
13. A.U. Abdurakhimov et al.: Yad. Fiz. **18**, 545 (1973); Nucl. Phys. **B79**, 57 (1974)
14. N. Angelov et al.: Yad. Fiz. **25**, 1013 (1977)
15. R.F. Schwitters et al.: Phys. Rev. Lett. **35**, 1320 (1975); G.G. Hanson et al.: Phys. Rev. Lett. **35**, 1609 (1975)
16. Ch. Berger et al.: Phys. Lett. **78B**, 176 (1978); Phys. Lett **81B**, 410 (1979); **82B**, 449 (1979)
17. R. Brandelik et al.: Phys. Lett. **83B**, 261 (1979)
18. D. Barber et al.: Phys. Rev. Lett. **42**, 1113 (1979)
19. G. Wolf: DESY, 80/85, Sept. 1980; Int. Conf. on High Energy Physics, Geneva, Vol. 1, 220, (1979)
20. W. Kittel: Soft Hadron-Hadron Collisions in the Light of Hard Collisions. XVI. Int. Symp. on Multiparticle Dynamics, Kiryat Anavim, (1985)
21. G. Hanson: SLAC-PUB-1984, Sept. (1976)
22. P. Allen et al.: Nucl. Phys. **B214**, 369 (1983)
23. S.D. Drell, D.J. Levy, T. Yan: Phys. Rev. **187**, 2159 (1969); Phys. Rev. **D1**, 1617 (1970)
24. A.U. Abdurakhimov et al.: JINR, 1-6967, Dubna (1973); JINR, R1-7267, Dubna (1973); Yad. Fiz. **18**, 1251 (1973)
25. N. Angelov et al.: JINR, P1-81-5, Dubna (1981)
26. H. Oberlak: MPI-PAE/Exp. E1-110, September (1982)
27. G. Wolf: DESY 81-086, December 1984
28. E. Balea et al.: Nucl. Phys. **B163**, 21 (1980)
29. K. Jaeger, D. Colley, L. Hyman, J. Rest: Phys. Rev. **D11**, 2405 (1975)
30. H. Kichimi et al.: Phys. Rev. **D20**, 37 (1979)
31. V.V. Anisovich, V.M. Shekhter: Nucl. Phys. **B55**, 455 (1973)
32. R.P. Feynman: Photon-Hadron Interactions, M.: Mir, (1975)
33. V.G. Kartvelishvili, V.N. Roinishvili: Preprint HEPI, 81-14, Serpukhov, (1981)
34. V.G. Grishin et al.: Yad. Fiz. **38**, 687 (1983)
35. A.M. Baldin et al.: Yad. Fiz. **39**, 1215 (1984); JINR, E1-84-317, Dubna (1984)
36. A.I. Anoshin et al.: Yad. Fiz. **36**, 409 (1982)
37. N. Angelov et al.: Yad. Fiz. **25**, 350 (1977); Yad. Fiz. **24**, 732 (1976)
38. V.G. Grishin, L.A. Didenko, A.A. Kuznetsov, Z.V. Metreveli: Yad. Fiz. **41**, 371 (1985); JINR, P1-84-205, Dubna (1984)
39. A.M. Baldin: Nucl. Phys. **A434**, 695C (1985)
40. A.M. Baldin, L.A. Didenko: Brief Comm. JINR, No. 3, p. 5 (1984); A.M. Baldin et al.: JINR, E1-85-675, Dubna (1985); P1-85-820, Dubna (1985)
41. A.M. Baldin, L.A. Didenko: Brief Comm. JINR, No. 8, p. 5 (1985)
42. Y. Cho et al.: Phys. Rev. Lett. **31**, 413 (1973)